PR 237

COPY

Using the Mixed Newton-Euler Formulation in the Orientation Control of Flexibly Mounted Bodies

Russell D. Smith
Center for Electromechanics

William F. Weldon
Department of Mechanical Engineering and
Department of Electrical and Computer Engineering

Ben M. Rech
Center for Electromechanics

Thomas J. Connolly
Department of Mechanical Engineering

The University of Texas at Austin

NATO ASI Conference:
Computational Methods in Mechanisms
Bulgaria, June 16-28 1997.

Abstract

Extended bodies whose own flexibility may conditionally be neglected can often be faithfully treated directly by any of several formulations based on classical dynamics. Here, the mixed approach employing the Newton-Euler equations for centroidal body-fixed frames will be used, where the absolute angular orientation will be computed via the associated kinematic differential equations relating the rotation matrix with the angular velocity vector. As an example of the practical (but restricted) use of simplified classical methods - and of the computationally attractive mixed Newton-Euler ODE formulation - the mathematical model of the U.S. Army's MLRS-ILMS mechanical launcher is described which is automatically controlled to simultaneously rotate about nonintersecting, nominally vertical and horizontal axes when commanded to target absolute angular orientation coordinates.

Introduction

Accurately capturing the dynamics of extended bodies frequently implies a judicious system description which typically involves interactions of both rigid and flexible members; accurately controlling the orientation or position of such bodies through flexible transmission paths is additionally cumbersome. The issue of addressing the relative importance of flexibility, component by component, in a physical system to be modeled is a familiar one which is best guided by a complete, empirically validated physical description. Existing systems which enjoy measurement and nominally defined operating conditions expedite a faithful analysis which can only remain tentative for systems still to be designed and built. While spacial dynamic analysis involving completely rigid constraints usually leads to a system of (hopefully solvable) differential algebraic equations (DAEs), the freedom of unconstrained motion of more general, flexibly mounted bodies, however, often yields the opportunity to shift attention back to a dynamic model highlighted by ODEs. To that end, the mixed dynamic-kinematic approach which retains the first-order form of the angular equations of motion will be presented.

Problem Formulation

The U.S. Army's MLRS ballistic platform is to be automatically controlled by hydraulic servomotors to simultaneously rotate about nonintersecting, nominally vertical (azimuth) and horizontal (elevation) axes. Figures 1 and 2 depict the launch platform under consideration: a large, tracked vehicle with a rectangular cage of rockets (or guided missiles, etc.) which is to be rotated about a horizontal (elevation) axis and a vertical (azimuth) axis simultaneously (each axis referenced with respect to the vehicle) as it moves toward commanded absolute angular orientation coordinates. As depicted in the simplified block diagram of Figure 3, a control signal current is fed to the servovalve of the elevation hydraulic servomotor (variable displacement) which produces a torque to be applied through an elevation transmission, ultimately manifesting itself as an elongation (or retraction) of the two ball screw actuators to elevate (or lower) the cage. Analogously, the azimuth drive (attached to a rigid, flexibly mounted base) operates on a control signal current to the servovalve of the variable displacement azimuth motor which produces torque through a transmission unit which acts against a ring gear mounted directly to the turret. Thus, it is the *turret* which is controlled through the azimuth transmission, the extended cage being mounted to the turret through two ball screws and two hinges along the pivoting (elevation) axis. It is to be emphasized, with reference to Figure 2, that the mass of the turret contributes toward the moment of inertia of the total cage assembly about the azimuth bearing axis, but does not contribute to the cage assembly's moment of inertia about the elevation axis. Of course, the moments about each of these critical axes will change discontinuously as the mass of the cage becomes depleted through firing, and - additionally - the cage/turret assembly moment of inertia about the azimuth axis is a nonnegligible function of the elevation angle (being reduced during elevation by as much as 25% from its maximum, "stowed" configuration value). The system as described above captures some of the essential features of what will become the ILMS, or Improved Launcher Mechanical System, as a result of the ongoing program to enhance the existing fleet of MLRS (Multiple Launch Rocket System) launchers.

Cage disturbance effects due to the firing of rockets involve a rather complicated sequence of events which begins with a sufficient thrust build-up (acting against launch tubes, in the forward direction) to shear the detent bolts holding the rocket in its launch tube. The ejection

Nomenclature

I_c	= cage inertia matrix	m	= cage mass
$\underline{h}^c$	= cage angular momentum	$\underline{\omega}^c$	= cage angular velocity
$\underline{F}_i^{BS}$	= ball screw force i acting on cage	ℓ	= $(\ell_{cmd} + \ell_{act})/2$
$\underline{F}_i^{hp}$	= hinge point force i acting on cage	K_i^{hp}	= stiffness matrix / hingepoint i
$\underline{F}^{Grav}$	= gravitational force acting on cage cm	ℓ_{act}	= actual length of ball screw
$\underline{F}^{rkt}$	= force acting on cage due to rocket	A_t	= turret rotation matrix
$k(\ell)$	= length-dependent ball screw stiffness	C_i^{hp}	= damping matrix / hingepoint i
A_c	= cage rotation matrix	ℓ_{cmd}	= commanded length of ball screw
A_t, A_b	= turret, base rotation matrices	θ, ψ	= absolute cage elev., azim. angles
λ	= ball screw pitch	ϕ	= rotational angle of ball screw
$\underline{r}_i^c$	= pos. vector from cage cm to cage point i	ω_m	= rotational speed of hyd. motor
$\underline{f}_i^c$	= force acting on cage point i (expressed locally)		
$\underline{F}_i^c$	= force acting on cage point i (expressed globally)		
$\underline{R}_{cm}^c$	= pos. vector of cage cm (expressed globally)		
$\underline{r}_i^t$	= pos. vector from turret bearing center to turret point i		
$\underline{R}_{brg}^t$	= pos. vector of turret brg (expressed globally)		
$\Delta\underline{R}_i^{hp}$	= displacement (globally expressed) between turret and cage of hingepoint i		

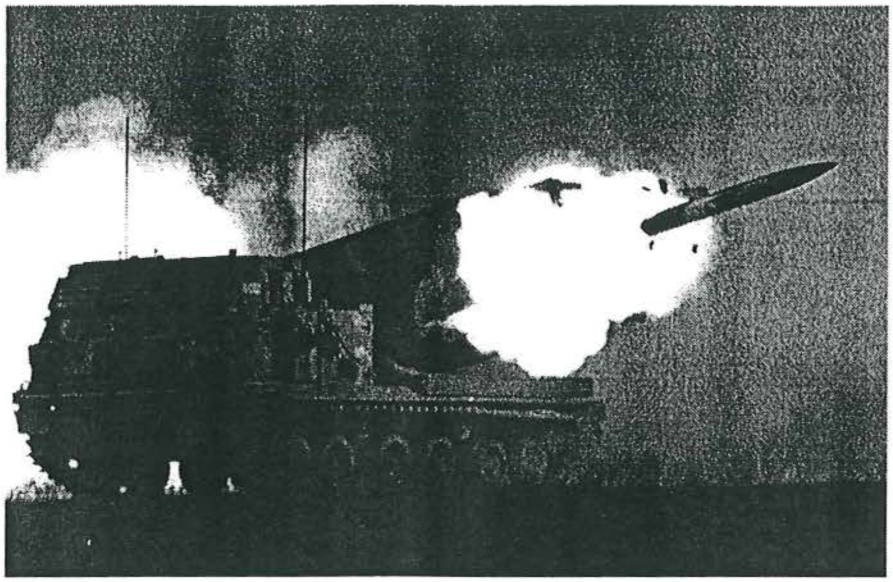

Figure 1: MLRS Launcher

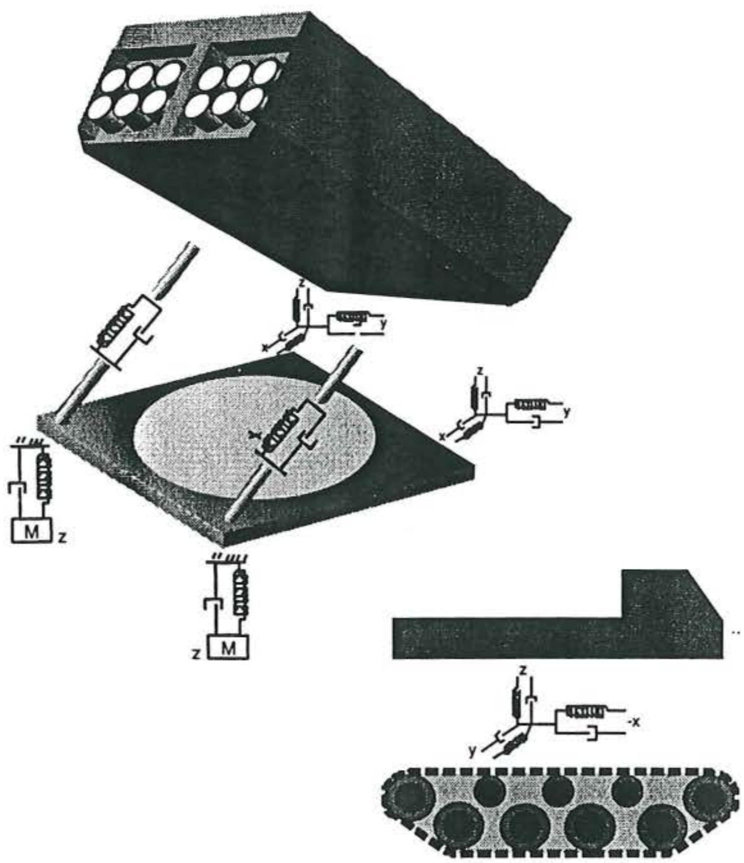

Figure 2: Mechanical Assembly Model

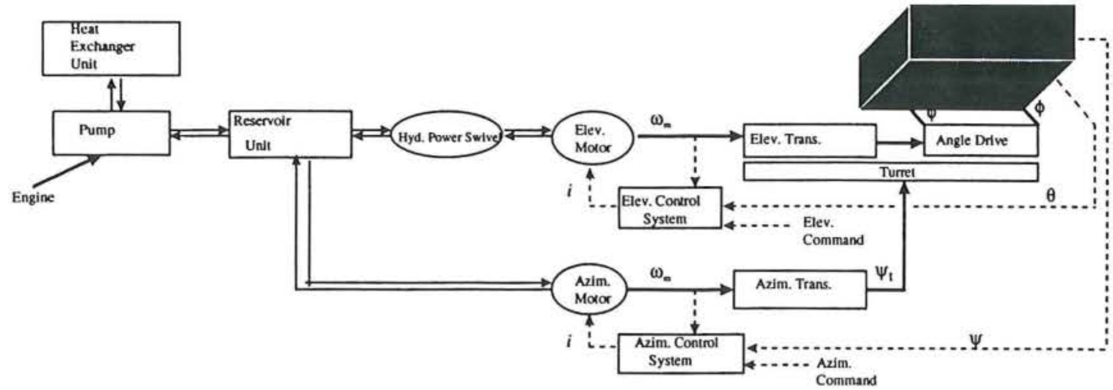

Figure 3: Simplified ILMS Block Diagram

of the rocket is then precipitated by a continuously changing inertia matrix ($I_c = I_{c(t)}$) as the fired rocket travels along the spin rails of the launch tubes prior to achieving free flight. The advent of rocket free flight implies a discontinuity in the cage inertia matrix at the instant that the rocket loses contact with the interior spin rails of the cage. The fired rocket then exerts blast forces on the exposed face of the cage due to its trailing plume which are considerable (approximately twice cage weight), but of brief duration. Under normal operation, the transient flexible modes of the system are permitted to damp out between firings (reaiming). Although there are aspects of cage and/or rocket motion which may depend upon a consideration of cage flexibility and which we will discuss below, the gross characteristics of interest here (with respect to normal aiming/firing scenarios) invite a rigid body treatment. However, the turret possesses considerable flexibility, especially in the vertical direction at the corners of attachment with the ball screws, and the hingepoint corners themselves will also be characterized by stiffness and damping in the three principal directions (locally oriented with turret's body-fixed axes). Thus, the cage is permitted six degrees-of-freedom in view of its flexible mounting.

A comprehensive, time-domain system description often becomes indispensable to the competent synthesis of a feedback control system, especially with regard to hydraulic control action with performance demands at the extremes of temperature experienced by military equipment. Such a time-domain system description is also necessary when addressing such effects as time delays, measurement noise, hysteresis, backlash, and failure analysis scenarios. These were some of the features of interest which motivated the comprehensive system model developed. It is with the treatment of rigid body cage/base motion that classical mechanics was blended with the approximate methods of discrete, or lumped parameter system dynamics analysis in an effort to produce a closed-loop set of state equations. Thus, given an adequate system dynamics which treats the elevation path from control signal input to ball screw extension as well as the azimuth path from control signal input to turret rotation, one is left to consider the mechanical assembly itself.

Dynamic Model

Cage

Provided that an appropriate control signal current is supplied to the servovalve of the (variable displacement) elevation hydraulic servomotor, the dynamics of the motor result in an applied torque which acts through a transmission to extend or contract the screws. Given the nominal lengths and the pitches of the ball screws, the *commanded* lengths are kinematically related to the angles through which the screws have turned. The ball screw/turret attachment points - having been described as turret mass-spring-dampers - each have position (and velocity) state variables associated with them. Thus, the cage being rigid, all points on or in the cage may be obtained by transforming suitable local frame, centroidal body-fixed cage vectors into equivalent global frame expressions through use of Eq. (3), where the reader is reminded that the reference point $\underline{R}^c_{cm}$ is dependent upon rocket configuration (i.e., changes with firing). The *actual* lengths of the ball screws, then, are obtained by vector subtraction of the endpoints of the screws. For ball screws which can be treated as flexible *axial* links, the forces generated may be obtained by multiplying the length-dependent variable stiffness against the difference between actual and commanded length. The lines of action of the forces are here approximated as collinearly directed between the known endpoints.

The four points at which the turret is attached to the cage are driven through a known angle by the azimuth motor (determined from the solution of the turret dynamics); superimposed on this circular motion is the flexure induced by ball screw forces (coriolis components being negligible), as well as the base vibration transmitted through the turret bearing. Again, the cage being rigid, its elevation hinge attachment points (refer Figure 2) are always available via Eq. (3). Thus, the vector component differences of the two hinge attachment points between cage and turret supply the components of differential motion which are suitably multiplied against turret corner stiffnesses calculated from an FEM analysis of the turret. The lines of action of these forces are similarly obtained from the known points on the cage and turret. Gravitational loading and rocket disturbance forces are also applied, their representations being inherently expressed in the global (inertial) and local (body-fixed) frames, respectively.

$$m\ddot{\underline{R}}^c_{cm} = \sum \underline{F}^c_i = \underline{F}^{BS}_i + \underline{F}^{hp}_i + \underline{F}^{Grav} + \underline{F}^{rkt} \tag{1}$$

$$\dot{\underline{h}}^c = (I_c\dot{\underline{\omega}}^c + \dot{I}_c\underline{\omega}^c) + \underline{\omega}^c \times \underline{h}^c = \sum (\underline{r}^c_i \times \underline{f}^c_i) = \sum (\underline{r}^c_i \times A^T_c \underline{F}^c_i) \tag{2}$$

In Eq. (1), the global (inertial) reference frame (for cartesian expression of position, velocity) is taken as fixed to the ground surface at the nose of the vehicle cab, while the centroidal, body-fixed frame for Eq. (2) is a rectangular frame which is nominally parallel with the global frame when the cage is in the "stowed" configuration. That is, for centroidal, body-fixed frames:

$$\underline{R}^c_i = A_c\underline{r}^c_i + \underline{R}^c_{cm} \tag{3}$$

$$\underline{f}^c_i = A^T_c\underline{F}^c_i \tag{4}$$

indicate the rotation matrix relation of an appropriate Euler angle set between frames for position and free vectors which are being taken with respect to Eqs. (1) and (2). The skew-symmetric matrix representation of the angular velocity of the cage (as expressed in its centroidal, body-fixed frame) is related to A_c through:

$$\underline{\tilde{\omega}}^c = \underline{\omega}^c \times = \begin{bmatrix} 0 & -\omega_z^c & \omega_y^c \\ \omega_z^c & 0 & -\omega_x^c \\ -\omega_y^c & \omega_x^c & 0 \end{bmatrix} = A_c^T \dot{A}_c \tag{5}$$

which implies the following matrix kinematic ODEs (among other forms):

$$\dot{A}_c = A_c \underline{\tilde{\omega}}^c \tag{6}$$

or,

$$\ddot{A}_c = A_c(\dot{\underline{\tilde{\omega}}} - \dot{A}_c^T \dot{A}_c) \tag{7}$$

Of the right hand side forces appearing in Eqs. (1) and (2), the directions and magnitudes of the rocket force and gravitational force are known, while the ball screw forces and damped elastic forces at the hingepoint corners of the turret may be obtained as follows:

$$\underline{F}_i^{BS} = k(t)(\ell_{cmd} - \ell_{act}) = k(t)(\lambda\phi - [(A_c \underline{r}_i^c + \underline{R}_{cm}^c) - (A_t \underline{r}_i^t + \underline{R}_{brg}^t)]) \tag{8}$$

Taking the differential displacement and velocity (as expressed in the global, fixed frame) between the cage and turret of an elevation axis hingepoint as:

$$\Delta\underline{R}_i^{hp} = [(A_c \underline{r}_i^c + \underline{R}_{cm}^c) - (A_t \underline{r}_i^t + \underline{R}_{brg}^t)] \tag{9}$$

$$\Delta\dot{\underline{R}}_i^{hp} = [(\dot{A}_c \underline{r}_i^c + \dot{\underline{R}}_{cm}^c) - (\dot{A}_t \underline{r}_i^t + \dot{\underline{R}}_{brg}^t)] \tag{10}$$

then the damped elastic forces acting upon the cage, as expressed globally, are:

$$\underline{F}_i^{hp} = A_t K_i^{hp}(A_t^T \Delta\underline{R}_i^{hp}) + A_t C_i^{hp}(A_t^T \Delta\dot{\underline{R}}_i^{hp}) \tag{11}$$

where K_i^{hp}, C_i^{hp} are the diagonal matrices characterizing the stiffness and damping of a hingepoint corner of the turret as determined from FEM analysis.

Although in Eq. (2) the explicit time-dependence of the cage inertia matrix has been noted, the numerical data describing the physical system is not refined enough (esp. products of inertia, rocket contact forces acting on cage, chassis suspension stiffnesses, etc.) to distinguish the contribution from rocket motion along the launch tubes prior to free flight, and that term is thus neglected.

Turret/Base

Formulations analogous to Eqs. (1) - (7) are applied to the 6 DOF, flexibly mounted base upon which the turret rotates (refer Figure 2), where the external forces and moments (in addition to the gravitational force) which act against it are transmitted either from the turret itself, through its large bearing, or by the stiffness and damping of the base suspension. Depending upon the firing orientation, any of the roll, pitch, or yaw modes of base motion may be excited by the forces transmitted through the turret. The turret has been modeled as a plate rotating about its azimuth bearing axis with respect to the base, with a moment of inertia which depends upon elevation angle. Additionally, the two turret corners of ball screw attachment are permitted to flex in the locally vertical direction only (in the frame of the turret). Thus,

$$A_t = \begin{bmatrix} \cos\psi_t & \sin\psi_t & 0 \\ -\sin\psi_t & \cos\psi_t & 0 \\ 0 & 0 & 1 \end{bmatrix} A_b \tag{12}$$

Controlled Response

Figure 4 is a plot of the elevation and azimuth angles of the cage, as provided by the global orientation of a nominal, body-fixed "pointing" vector continuously transformed through Eq. (3). In the figure, a 90° azimuth angle and a 57° elevation angle have been commanded, but azimuth motion is not permitted owing to geometric limitations until the cage has cleared the cab (see Figure 1) at approximately 17° elevation. Figure 5 indicates the approximate axial forces which the ball screws experience while elevating the cage. They are of relatively large magnitude at low angles of elevation where the mechanical advantage is least, and vice versa. The plots shown represent a fully loaded launcher resting on *level* ground, thus the numerical values of ball screw force represent that magnitude of loading carried in each ball screw; that is, the curves for the two ball screws cannot be distinguished at the scale shown. Under general, more highly asymmetric loading, separation would be evident.

As a further indication of the mixed Newton-Euler formulation of the cage/turret/base multibody dynamics, a simultaneous braking event of elevation and azimuth motion is shown in Figures 6 and 7, where "sudden" braking has been implemented in the form of kinematically locking the respective hydraulic motor shafts ($\omega_m = 0$), which, in the azimuth drive, is equivalent to locking the turret. The 3.5 Hz elevation oscillation propagated in Figure 6 is characteristic of elevation path flexibility, while the instantaneous braking event excites higher order contributions of azimuth path flexibility from the stiff hingepoints along the elevation axis.

Discussion

Using the mixed Newton-Euler ODE formulation avoids the DAE system implied by the introduction of the Euler parameters and their normalization constraint. Depending upon other system dynamics, which might influence (or dictate) the numerical solution approach, this difference may be significant; for example, logic intensive models are notoriously sensitive to the integration algorithm chosen.

One can imagine modes of operation of the system in which a rigid body treatment of the cage assembly, as was presented here, might be less persuasive. The actual method of fabrication of the components obviously plays a role in this issue, but, moreover, one must always bear in mind the use for which the model is intended. As was already mentioned, under normal operation of the existing MLRS launcher, pauses between rounds are required to permit the transient flexible system modes to damp out; such will also be the case with the ILMS launcher. However, the pursuit of failure mode scenarios involving braking maneuvers with an empty cage under steep ground slope conditions may well invalidate rigid treatments. Also, attempts to predict the initial conditions of the rocket (in contrast to cage dynamics) for use with trajectory simulations involve complicated rocket interaction effects with the spin rails of the cage's launch tubes which raise questions about the flexure effects on the rocket.

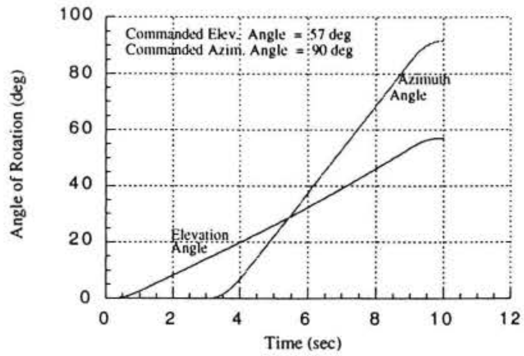

Figure 4: Cage Path Trajectory

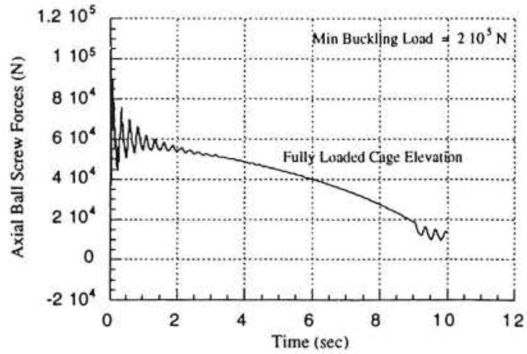

Figure 5: Ball Screw Actuator Forces

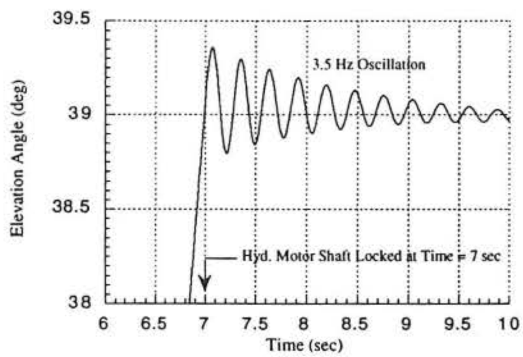

Figure 6: Elevation Braking

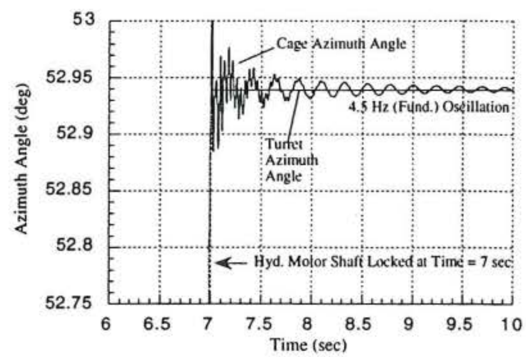

Figure 7: Azimuth Braking

Acknowledgements

The authors wish to extend their thanks to the U.S. Army Missile Command and the MLRS Project Office at Redstone Arsenal, Alabama. They also wish to thank Lockheed-Martin Vought Systems.

References

[1] A. F. D'Souza and V. K. Garg, *Advanced Dynamics: Modeling and Analysis*, Prentice-Hall, 1984.

[2] D. T. Greenwood, *Principles of Dynamics*, Prentice-Hall, 2nd Ed., 1988.

[3] E. J. Haug, *Intermediate Dynamics*, Prentice-Hall, 1992.

[4] P. Dransfield, *Hydraulic Control Systems - Design and Analysis of Their Dynamics*, Vol. 33 of Lecture Notes in Control and Information Sciences, Ed. by A. V. Balakrishnan and M. Thoma, Springer-Verlag, 1981.

[5] R. C. Rosenberg and D. C. Karnopp, *Introduction To Physical System Dynamics*, McGraw-Hill, 1983.

[6] H. E. Merritt, *Hydraulic Control Systems*, John Wiley & Sons, 1967.

[7] E. J. Haug, Editor, *Computer Aided Analysis and Optimization of Mechanical System Dynamics*, Springer-Verlag, 1984.